

# Redox Activity of Pyridine-Oxazoline Ligands in the Stabilization of Low-Valent Organonickel Radical Complexes

Clifton L. Wagner,<sup>†</sup> Gabriel Herrera,<sup>†</sup> Qiao Lin, Chunhua T. Hu, and Tianning Diao\*

Cite This: *J. Am. Chem. Soc.* 2021, 143, 5295–5300

Read Online

ACCESS |

Metrics & More

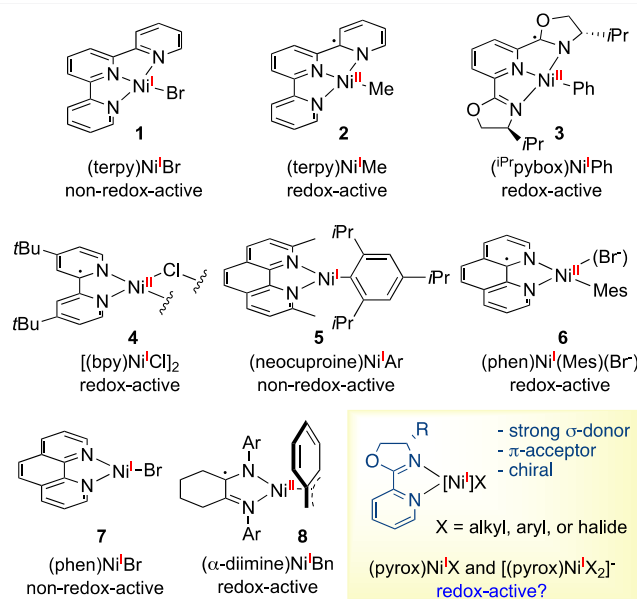
Article Recommendations

Supporting Information

**ABSTRACT:** Low-valent organonickel radical complexes are common intermediates in cross-coupling reactions and metalloenzyme-mediated processes. The electronic structures of *N*-ligand supported nickel complexes appear to vary depending on the actor ligands and the coordination number. The reduction products of a series of divalent (pyrox)Ni complexes establish the redox activity of pyrox in stabilizing electron-rich Ni(II)–alkyl and –aryl complexes by adopting a ligand-centered radical configuration. The reduced pyrox imparts an enhanced *trans*-influence. In contrast, such redox activity was not observed in a (pyrox)Ni(I)–bromide species. The excellent capability of pyrox in stabilizing electron-rich Ni species resonates with its proclivity in promoting the reductive activation of C(sp<sup>3</sup>) electrophiles in cross-coupling reactions.

The rapid advancement of nickel-catalyzed cross-coupling reactions has been accompanied by the evolution of ligands to promote substrate activation, stabilize reaction intermediates, tune reaction selectivity, and facilitate bond formation processes.<sup>1–5</sup>  $\sigma$ -Donor ligands, including phosphines and *N*-heterocyclic carbenes (NHC), have been frequently applied to reactions involving two-electron redox pathways proceeding through Ni(0)/Ni(II) cycles.<sup>6</sup> Reactions invoking radical pathways often employ bidentate and tridentate *N*-ligands, such as bis(oxazolinylpyridine) (pybox),<sup>7</sup> terpyridine (terpy),<sup>8–10</sup> bipyridine (bpy), and analogues,<sup>11</sup> bis-oxazoline (box),<sup>12,13</sup> 2,2'-linked bioxazoline (biOx),<sup>14,15</sup> and pyridine-oxazoline (pyrox) ligands.<sup>16–20</sup> These ligands are strong  $\sigma$ -donors<sup>21</sup> as well as  $\pi$ -acceptors, leading to high field splitting and excellent stabilization of open-shell organometallic intermediates.

Open-shell, low-valent organometallic Ni complexes, ligated with *N*-chelating ligands, have been extensively proposed as key intermediates in cross-coupling reactions as well as metalloenzyme-mediated biological processes.<sup>22,23</sup> Characterization of the electronic structures of monovalent Ni complexes can shed light on the reaction mechanisms and inform ligand design principles. Seminal organometallic Ni(I) complexes consist of bulky phosphine<sup>24–27</sup> and NHC ligands.<sup>28</sup> The redox activity of the more catalytically relevant *N*-donor ligands appears to vary depending on the actor ligands and the coordination number of the nickel center. A switch in the location of the unpaired electron between Ni and the ligand was first observed in (terpy)Ni complexes **1** and **2** (Figure 1).<sup>29</sup> A (pybox)Ni(Ph) complex **3** is best described as a divalent Ni(II) stabilized by a pybox radical anion.<sup>30</sup> (Bpy)Ni analogues **4–7** accommodate various electronic structures.<sup>31–36</sup> The redox activity of  $\alpha$ -diimine ligands has been established in a number of Ni complexes, such as **8**.<sup>37–39</sup> A (Phbox)Ni(Br) complex exhibits predominantly metalloradical character due to the lack of conjugation between the two oxazoline rings.<sup>40</sup>



Common intermediates proposed in cross-coupling reactions

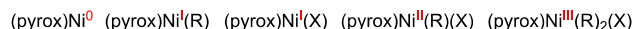


**Figure 1.** Low-valent organonickel radical complexes bearing chelating *N*-ligands and their electronic structures. The compound formula and formal oxidation states are shown underneath each structure, whereas the assigned oxidation states of nickel and the ligands are labeled in the structures based on spectroscopic characterizations.

Received: January 16, 2021

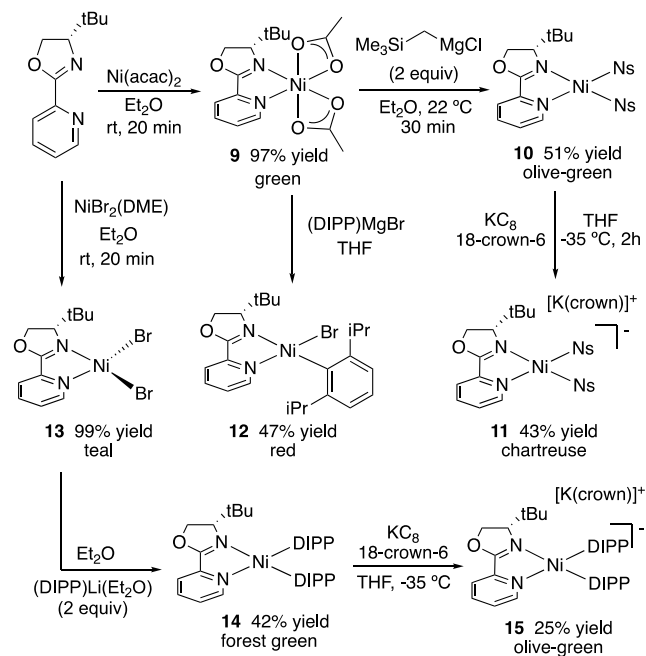
Published: April 1, 2021



Pyrox, including the readily available chiral variants, is a versatile ligand for promoting the reductive Heck reaction<sup>17</sup> and asymmetric cross-coupling of C(sp<sup>3</sup>) partners, in particular.<sup>16,18,19</sup> Compared to pybox, bidentate pyrox may be more capable of accommodating high-valent species (Figure 1). Among bidentate ligands, the C1 symmetric pyrox poses a “push–pull” effect by the oxazoline and pyridine moieties that facilitate oxidative addition as well as reductive elimination.<sup>41</sup> Although being implied in a rhenium complex,<sup>42</sup> the redox activity of pyrox ligands has not been characterized in the context of stabilizing open-shell transition metal complexes. The prevalence of monovalent (pyrox)Ni intermediates in catalysis, the versatile electronic structures of N-ligated Ni radical complexes, and the dearth of knowledge in the redox activity of pyrox prompted us to investigate the redox activity of pyrox in stabilizing low-valent nickel-alkyl, aryl, and bromide complexes.

We selected (*S*)-<sup>t</sup>Bu pyrox as a platform for preparing (pyrox)Ni model complexes (Scheme 1). Transmetalation of

### Scheme 1. Syntheses of ((*S*)-<sup>t</sup>BuPyrox)Ni(II) and Ni(I) Complexes



(<sup>t</sup>Bu pyrox)Ni(acac)<sub>2</sub> **9** (acac = acetylacetonate) with neosilylmagnesium chloride generated (<sup>t</sup>Bu pyrox)Ni(Ns)<sub>2</sub> **10** (Ns = neosilyl) as an olive green crystal. Addition of (DIPP) magnesium bromide (DIPP = 2,6-diisopropylphenyl) to **9** afforded **12** in 47% yield. (<sup>t</sup>Bu pyrox)NiBr<sub>2</sub> **13** was conveniently prepared by combining (*S*)-<sup>t</sup>Bu pyrox and NiBr<sub>2</sub>(DME). Treating **13** with 2 equiv of (DIPP)lithium gave (<sup>t</sup>Bu pyrox)Ni(DIPP)<sub>2</sub> **14** as a teal crystal. Complexes **10**, **12** and **14** are low-spin Ni(II) complexes, evident by their diamagnetic <sup>1</sup>H NMR spectra (Figures S1, S3, and S5) and the square-planar geometry as determined by single crystal X-ray diffraction (Figures S23, S25, and S26).

The cyclic voltammetry (CV) study of **10** and **14** reveals quasi-reversible redox waves corresponding to the redox couples of Ni(II)/Ni(I) (Figures S9 and S12). The data suggests modest stability of Ni(I) species, which prompted us to attempt the chemical reduction of **10** and **14**.<sup>43</sup> Treating **10**

with 1 equiv of potassium graphite (KC<sub>8</sub>) along with an equal molarity of 18-crown-6 in THF led to a chartreuse crystalline complex **11**.<sup>44</sup> Single crystal X-ray diffraction establishes the structure of **11** to be [K<sup>+</sup>(crown)][(<sup>t</sup>Bu pyrox)NiN<sub>2</sub>]<sup>-</sup> (Figure 2A). Performing a similar reduction of **14** led to the formation

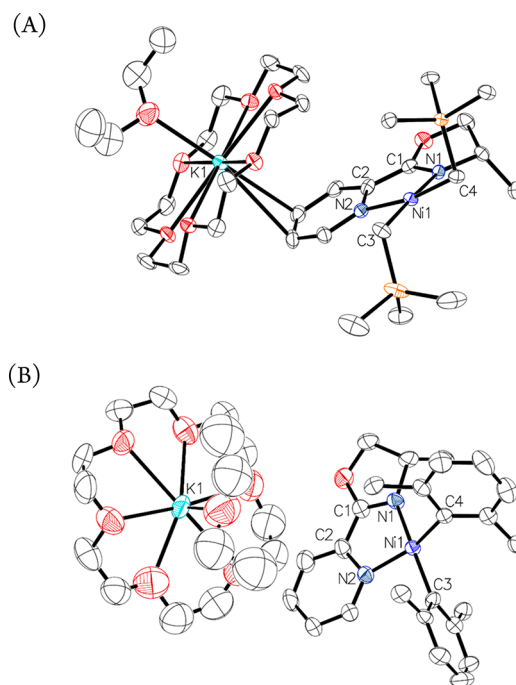


**Figure 2.** X-ray structures of Ni complexes **11** (A) and **15** (B) at 50% probability thermal ellipsoids. Hydrogen atoms are omitted, and *t*-Bu and isopropyl groups are truncated for clarity.

of [K<sup>+</sup>(crown)][(<sup>t</sup>Bu pyrox)Ni(DIPP)<sub>2</sub>]<sup>-</sup> **15** as an olive green complex, insoluble in Et<sub>2</sub>O (Figure 2B). Our attempts to reduce **12** under similar conditions resulted in rapid disproportionation to form **14** and Ni black.

Both anions **11** and **15** adopt a square planar geometry similar to that of the neutral **10** and **14** (Figure 2). In **11**, there is a secondary bonding interaction between the pyridine and [K(crown)]<sup>+</sup>, evident by a close distance between [K(crown)]<sup>+</sup> and two carbons of the pyridine (3.202(7) and 3.333(7) Å), whereas such interactions are absent in **15**. The bond lengths of the pyrox ligands are indicative of the redox state of the ligand.<sup>45</sup> Comparing complexes **11** with **10**, the N<sub>ox</sub>–C<sub>ox</sub> bond distance of 1.311(7) Å in **11** is longer than that of **10** (1.285(8) Å), the C<sub>ox</sub>–C<sub>pyr</sub> bond distance of 1.393(8) Å significantly shorter than 1.438(9) Å, and the C<sub>pyr</sub>–N<sub>pyr</sub> bond distance of 1.402(8) Å substantially longer than 1.360(9) Å (Table 1). These parameters reveal that the pyrox in **11** is reduced to [pyrox]<sup>•-</sup>. The bond lengths of complex **15** follow a similar trend compared to **12** and **14**, displaying elongated N<sub>ox</sub>–C<sub>ox</sub> and C<sub>pyr</sub>–N<sub>pyr</sub> bonds and a shorter C<sub>ox</sub>–C<sub>pyr</sub> bond, although the difference is less pronounced considering the error bars.

In **10** and **14**, the longer Ni–C(4) relative to Ni–C(3) reveals a stronger *trans*-influence of pyridine compared to oxazoline, giving rise to the “push–pull” effect, consequential in asymmetric catalysis.<sup>41</sup> The elongated Ni–C bonds, Ni–C(3) and Ni–C(4), in **11** and **15** relative to those of **10** and **14** substantiate an enhanced *trans*-influence of pyrox in the reduced form.

Table 1. Metrical Parameters of (*t*BuPyrox)Ni Complexes

complex	N <sub>ox</sub> -C <sub>ox</sub> (N(1)-C(1) Å)	C <sub>ox</sub> -C <sub>pyr</sub> (C(1)-C(2) Å)	C <sub>pyr</sub> -N <sub>pyr</sub> (C(2)-N(2) Å)	Ni-C(3) (Å)	Ni-C(4) (Å)
10	1.285(8)	1.438(9)	1.360(9)	1.925(7)	1.943(8)
11	1.311(7)	1.393(8)	1.402(8)	1.934(6)	1.952(6)
12	1.300(17)	1.441(18)	1.351(16)		
14	1.277(6)	1.452(7)	1.360(6)	1.909(5)	1.923(7)
15	1.317(12)	1.423(14)	1.378(12)	1.916(9)	1.940(9)

The EPR spectrum of **11** in a toluene solution at 295 K displays an isotropic signal with  $g_{\text{iso}} = 2.009$ , along with hyperfine coupling to two N donors ( $I = 1$ ) and three H atoms ( $I = 1/2$ ) (Figure 3A). At 10 K, the glassy frozen solution of **11**

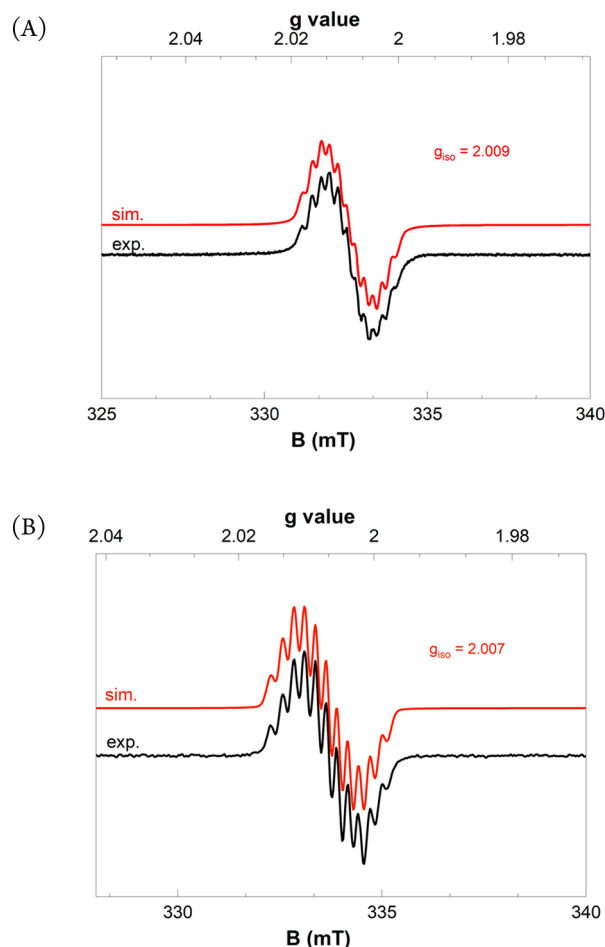


**Figure 3.** X-band EPR spectra of **11** (A) and **15** (B) (black). Temperature = 295 K, solvent = toluene. The simulated spectra (red) used the following parameters: **11**,  $g_{\text{iso}} = 2.009$ ,  $A_{\text{N,N,H,H,H}} = [7.0, 8.7, 8.2, 14.1, 22.4]$  MHz; **15**,  $g_{\text{iso}} = 2.007$ ,  $A_{\text{N,N,H,H,H}} = [7.6, 7.6, 7.3, 14.5, 21.3]$  MHz.

reveals a rhombic signal, which can be simulated by applying the parameters:  $g_x = 1.999$ ,  $g_y = 2.006$ ,  $g_z = 2.019$  (Figure S19). The average  $g$  value of 2.008 and the small anisotropy  $\Delta g$  of 0.020 are comparable to those of  $[(\text{bpy})\text{Ni}(\text{Mes})_2]^{•-}$ .<sup>31</sup> A similar isotropic EPR signal was recorded for **15** at 295 K (Figure 3B) and at 10 K (Figure S20). The isotropic EPR spectra of both **11** and **15** with  $g$  values close to 2.003, combined with the hyperfine coupling to two N atoms and three H atoms on the ligand, led us to assign the radical density to the ligand, with small nickel contribution. The reduction of **12** by  $\text{KC}_8$  resulted in an unstable species, the EPR spectrum

of which is consistent with an organic radical with a  $g$  value of 2.005 (Figure S21).

We performed geometry optimizations and single-point calculations at the B3LYP level, using the ORCA program.<sup>46</sup> The computed Mulliken spin density reveals that the unpaired electron is delocalized to the pyrox ligands in **11** and **15** (Figure 4). The DFT data is corroborated with the X-ray

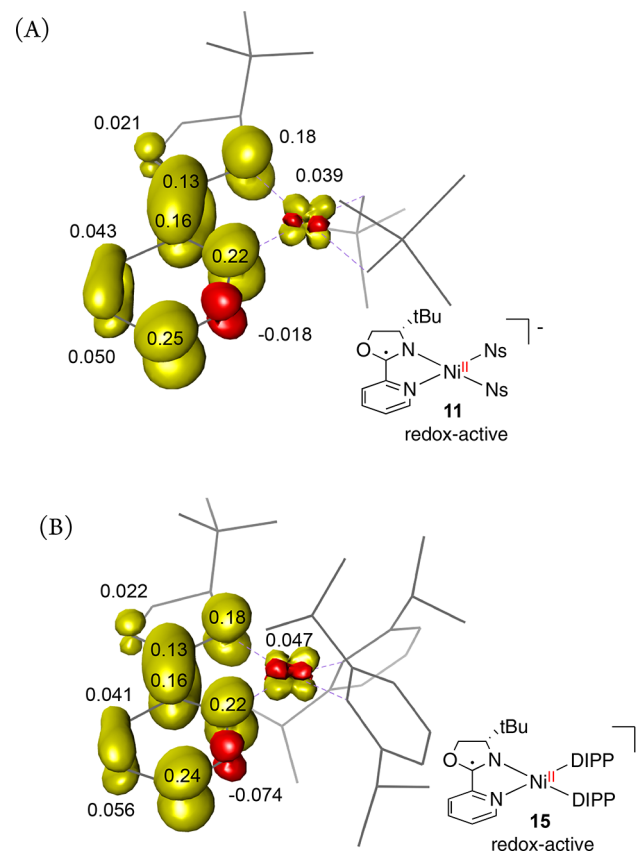
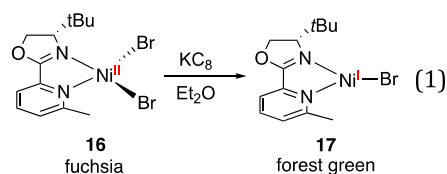


**Figure 4.** Spin density plots for **11** (A) and **15** (B) obtained from Mulliken population analysis.

structural characterization and the EPR spectra of **11** and **15**, establishing low-spin Ni(II)  $d^8$  species with a radical in the  $\pi^*$  orbital of pyrox.

Our attempts to reduce **13** resulted in rapid decomposition. The reduction of the bulky complex **16** by  $\text{KC}_8$  furnished a paramagnetic species, assigned to Ni(I) **17** (eq 1). EPR



analysis at 10 K gave rhombic signals, simulated with parameters  $g_x = 2.373$ ,  $g_y = 2.180$ , and  $g_z = 2.109$ , indicating a Ni-centered radical (Figure 5A). This assignment agrees with

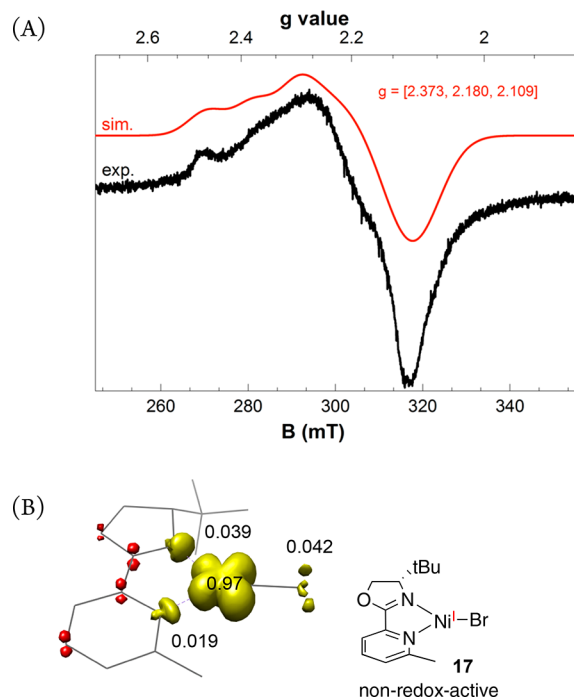


**Figure 5.** X-band EPR spectrum (A) and spin density plot of **17** (B). Temperature = 10 K, solvent = toluene. The simulated spectrum (red) uses the following parameters: **17**,  $g_x = 2.373$ ,  $g_y = 2.180$ ,  $g_z = 2.109$ ,  $A_{N_x} = 350$  MHz,  $A_{N_y} = 58$  MHz, and  $A_{N_z} = 0$  MHz.

the DFT calculations, in which the single point energy calculation converged to a solution with a spin-density of 0.97 on the nickel center (Figure 5B). The different electronic structures between **11**, **15** and **17** are reminiscent of those observed in (terpy)Ni<sup>29</sup> and (phen)Ni complexes.<sup>35</sup> We attribute the lack of ligand redox activity in **17** to the weaker electron-donating capability of bromide relative to aryl and neosilyl groups and the change of coordination number from four to three.

Nickelate complexes are resilient intermediates in cross-coupling reactions.<sup>47</sup> Ni(I)–aryl species have been proposed to activate alkyl halides to afford radicals, whereas Ni(I)–halide complexes preferentially react with aryl halides.<sup>36</sup> We explored the reactivity of **15** with a variety of alkyl and aryl halides (Table 2). Iodomethane immediately reacted with **15** to afford ethane and **14**. This result is consistent with single-electron activation of MeI by **15**, followed by methyl radical dimerization, while Ni(I) was oxidized to Ni(II). We attribute the poor mass balance of Ni to the instability of **14** and **15**. The activation of cyclopropylmethyl bromide by **15** gave **18**, raised from the dimerization of the homoallylic radical. Chlorocyclohexane and *para*-toluoyl bromide were inert toward **15**.

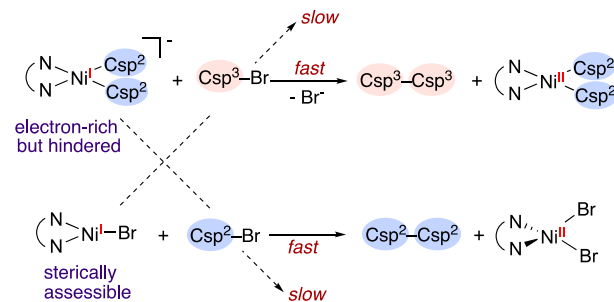
Ni(I) **17** displayed contrasting selectivity compared to **15**. Subjecting Csp<sup>3</sup> electrophiles, including iodomethane, cyclopropylmethyl bromide, and chlorocyclohexane, to **17** resulted in no radical dimerization product (Table 2). On the contrary, **17** reacted with *para*-toluoyl bromide to afford 4,4'-bitoluene in 33% yield and Ni(II) **16** in 59% yield.

**Table 2.** Reactivity of **15** and **17** with Electrophiles to Afford Radicals

		[Ni <sup>I</sup> ] + R-X $\xrightarrow[22\text{ }^\circ\text{C}]{\text{THF-}d_6}$ [Ni <sup>II</sup> ] + R-R $\left[ \begin{array}{c} \text{via} \\ \text{R}\cdot \end{array} \right]$	
		<b>15</b> or <b>17</b>	<b>14</b> or <b>16</b>
Electrophile	Ni(I) complex		
CH <sub>3</sub> -I		CH <sub>3</sub> -CH <sub>3</sub> (95% yield)	<b>14</b> (41% yield)
		 <b>18</b> (22% yield)	<b>14</b> (22% yield)
		no reaction	no reaction
		no reaction	<i>p</i> -Tol- <i>p</i> -Tol <b>16</b> (33% yield) (59% yield)

The preference of C(sp<sup>3</sup>) over C(sp<sup>2</sup>) electrophiles by **15** could stem from the high electron-density that facilitates electron transfer, whereas the large steric hindrance prevents the approach of Csp<sup>2</sup> electrophiles to the Ni center (Scheme 2). Ni(I)–Br complex **17** favors C(sp<sup>2</sup>) to C(sp<sup>3</sup>) electro-

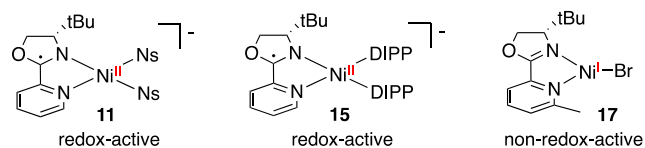
**Scheme 2.** Selectivity of Ni(I) Complexes in Activating Csp<sup>2</sup> and Csp<sup>3</sup> Electrophiles



philes, because the open geometry allows for oxidative addition of aryl bromides to the Ni(I) center. The difference in selectivity of Ni(I)–aryl and Ni(I)–Br species supports our previous proposal that C(sp<sup>2</sup>) and C(sp<sup>3</sup>) electrophiles are separately activated by Ni(I)–Br and Ni(I)–aryl species, respectively.<sup>36</sup> The sequential mechanism accounts for the chemoselectivity observed in cross-electrophile coupling reactions.

In summary, pyrox is redox-active in stabilizing **11** and **15** to give [pyrox]<sup>•-</sup> ligated low-spin d<sup>8</sup> Ni(II) species. Pyridine is a better donor than oxazoline. The unsymmetrical *trans*-influence between pyridine and oxazoline, enhanced in the reduced form, is consequential to stereochemical models for chiral induction. Complex **17**, in contrast, is a nickel-centered radical. The different electronic structures can be attributed to the electron-donating ability of the X ligands on Ni and the coordination number. Complexes **15** and **17** exhibit divergent activity between C(sp<sup>2</sup>) and C(sp<sup>3</sup>) electrophiles, which can account for the chemoselectivity in cross-electrophile coupling

reactions.<sup>36</sup> The stabilization of organonickel radical intermediates by the redox active pyrox contributes to their proclivity in activating C(sp<sup>3</sup>) electrophiles to afford radical intermediates, a reactivity that distinguishes nickel from palladium in cross-coupling reactions.<sup>4</sup>



## ASSOCIATED CONTENT

### Supporting Information

The Supporting Information is available free of charge at <https://pubs.acs.org/doi/10.1021/jacs.1c00440>.

All experimental procedures, additional figures, details of DFT calculations, and NMR spectra (PDF)

### Accession Codes

CCDC 2054558–2054563 contain the supplementary crystallographic data for this paper. These data can be obtained free of charge via [www.ccdc.cam.ac.uk/data\\_request/cif](http://www.ccdc.cam.ac.uk/data_request/cif), or by emailing [data\\_request@ccdc.cam.ac.uk](mailto:data_request@ccdc.cam.ac.uk), or by contacting The Cambridge Crystallographic Data Centre, 12 Union Road, Cambridge CB2 1EZ, UK; fax: +44 1223 336033.

## AUTHOR INFORMATION

### Corresponding Author

Tianning Diao – Department of Chemistry, New York University, New York 10003, United States; [orcid.org/0000-0003-3916-8372](https://orcid.org/0000-0003-3916-8372); Email: [diao@nyu.edu](mailto:diao@nyu.edu)

### Authors

Clifton L. Wagner – Department of Chemistry, New York University, New York 10003, United States

Gabriel Herrera – Department of Chemistry, New York University, New York 10003, United States

Qiao Lin – Department of Chemistry, New York University, New York 10003, United States

Chunhua T. Hu – Department of Chemistry, New York University, New York 10003, United States; [orcid.org/0000-0002-8172-2202](https://orcid.org/0000-0002-8172-2202)

Complete contact information is available at: <https://pubs.acs.org/doi/10.1021/jacs.1c00440>

### Author Contributions

<sup>†</sup>C.L.W. and G.H. contributed equally.

### Notes

The authors declare no competing financial interest.

## ACKNOWLEDGMENTS

This work was supported by the National Institutes of Health (NIH) under Award Number R01GM127778 and the diversity supplement program for C.L.W. T.D. is a recipient of the Alfred P. Sloan Research Fellowship (FG-2018-10354) and the Camille-Dreyfus Teacher-Scholar Award (TC-19-019). T.D. acknowledges NSF (1827902) for funding to acquire the EPR spectrometer. The X-ray facility was supported partially by the National Science Foundation (NSF) (CHE-0840277 and DMR-1420073).

## REFERENCES

- Hu, X. Nickel-catalyzed cross coupling of non-activated alkyl halides: a mechanistic perspective. *Chem. Sci.* **2011**, *2*, 1867–1886.
- Tasker, S. Z.; Standley, E. A.; Jamison, T. F. Recent Advances in Homogeneous Nickel Catalysis. *Nature* **2014**, *509*, 299–309.
- Fu, G. C. Transition-Metal Catalysis of Nucleophilic Substitution Reactions: A Radical Alternative to S<sub>N</sub>1 and S<sub>N</sub>2 Processes. *ACS Cent. Sci.* **2017**, *3*, 692–700.
- Diccianni, J.; Diao, T. Mechanisms of Nickel-Catalyzed Cross Coupling Reactions. *Trends Chem.* **2019**, *1*, 830–844.
- Diccianni, J.; Lin, Q.; Diao, T. Mechanisms of Nickel-Catalyzed Cross Coupling Reactions and Applications in Alkene Functionalization. *Acc. Chem. Res.* **2020**, *53*, 906–919.
- Rosen, B. M.; Quasdorf, K. W.; Wilson, D. A.; Zhang, N.; Resmerita, A.-M.; Garg, N. K.; Percec, V. Nickel-Catalyzed Cross-Couplings Involving Carbon–Oxygen Bonds. *Chem. Rev.* **2011**, *111*, 1346–1416.
- Zhou, J.; Fu, G. C. Cross-Couplings of Unactivated Secondary Alkyl Halides: Room-Temperature Nickel-Catalyzed Negishi Reactions of Alkyl Bromides and Iodides. *J. Am. Chem. Soc.* **2003**, *125*, 14726–14727.
- Anderson, T. J.; Jones, G. D.; Vivic, D. A. Evidence for a Ni<sup>I</sup> Active Species in the Catalytic Cross-Coupling of Alkyl Electrophiles. *J. Am. Chem. Soc.* **2004**, *126*, 8100–8101.
- Jones, G. D.; Martin, J. L.; McFarland, C.; Allen, O. R.; Hall, R. E.; Haley, A. D.; Brandon, R. J.; Konovalova, T.; Desrochers, P. J.; Pulay, P.; Vivic, D. A. Ligand Redox Effects in the Synthesis, Electronic Structure, and Reactivity of an Alkyl–Alkyl Cross-Coupling Catalyst. *J. Am. Chem. Soc.* **2006**, *128*, 13175–13183.
- Gong, H.; Gagné, M. R. Diastereoselective Ni-Catalyzed Negishi Cross-Coupling Approach to Saturated, Fully Oxygenated C-Alkyl and C-Aryl Glycosides. *J. Am. Chem. Soc.* **2008**, *130*, 12177–12183.
- Everson, D. A.; Shrestha, R.; Weix, D. J. Nickel-Catalyzed Reductive Cross-Coupling of Aryl Halides with Alkyl Halides. *J. Am. Chem. Soc.* **2010**, *132*, 920–921.
- Lou, S.; Fu, G. C. Nickel/Bis(oxazoline)-Catalyzed Asymmetric Kumada Reactions of Alkyl Electrophiles: Cross-Couplings of Racemic  $\alpha$ -Bromoketones. *J. Am. Chem. Soc.* **2010**, *132*, 1264–1266.
- Hofstra, J. L.; Cherney, A. H.; Ordner, C. M.; Reisman, S. E. Synthesis of Enantioenriched Allylic Silanes via Nickel-Catalyzed Reductive Cross-Coupling. *J. Am. Chem. Soc.* **2018**, *140*, 139–142.
- Do, H.-Q.; Chandrashekar, E. R. R.; Fu, G. C. Nickel/Bis(oxazoline)-Catalyzed Asymmetric Negishi Arylations of Racemic Secondary Benzylic Electrophiles to Generate Enantioenriched 1,1-Diaryllkanes. *J. Am. Chem. Soc.* **2013**, *135*, 16288–16291.
- Tellis, J. C.; Primer, D. N.; Molander, G. A. Single-electron transmetalation in organoboron cross-coupling by photoredox/nickel dual catalysis. *Science* **2014**, *345*, 433.
- Binder, J. T.; Cordier, C. J.; Fu, G. C. Catalytic Enantioselective Cross-Couplings of Secondary Alkyl Electrophiles with Secondary Alkylmetal Nucleophiles: Negishi Reactions of Racemic Benzylic Bromides with Achiral Alkylzinc Reagents. *J. Am. Chem. Soc.* **2012**, *134*, 17003–17006.
- Zhou, F.; Zhu, J.; Zhang, Y.; Zhu, S. NiH-Catalyzed Reductive Relay Hydroalkylation: A Strategy for the Remote C(sp<sup>3</sup>)–H Alkylation of Alkenes. *Angew. Chem., Int. Ed.* **2018**, *57*, 4058–4062.
- Qiu, H.; Shuai, B.; Wang, Y.-Z.; Liu, D.; Chen, Y.-G.; Gao, P.-S.; Ma, H.-X.; Chen, S.; Mei, T.-S. Enantioselective Ni-Catalyzed Electrochemical Synthesis of Biaryl Atropisomers. *J. Am. Chem. Soc.* **2020**, *142*, 9872–9878.
- Huo, H.; Gorsline, B. J.; Fu, G. C. Catalyst-controlled doubly enantioconvergent coupling of racemic alkyl nucleophiles and electrophiles. *Science* **2020**, *367*, 559–564.
- Li, Y.; Li, Y.; Peng, L.; Wu, D.; Zhu, L.; Yin, G. Nickel-catalyzed migratory alkyl–alkyl cross-coupling reaction. *Chem. Sci.* **2020**, *11*, 10461–10464.

- (21) Van Hecke, G. R.; Horrocks, W. D. Approximate Force Constants for Tetrahedral Metal Carbonyls and Nitrosyls. *Inorg. Chem.* **1966**, *5*, 1960–1968.
- (22) Lin, C.-Y.; Power, P. P. Complexes of Ni(I): a "rare" oxidation state of growing importance. *Chem. Soc. Rev.* **2017**, *46*, 5347–5399.
- (23) Zimmermann, P.; Limberg, C. Activation of Small Molecules at Nickel(I) Moieties. *J. Am. Chem. Soc.* **2017**, *139*, 4233–4242.
- (24) Kitiachvili, K. D.; Mendiola, D. J.; Hillhouse, G. L. Preparation of Stable Alkyl Complexes of Ni(I) and Their One-Electron Oxidation to Ni(II) Complex Cations. *J. Am. Chem. Soc.* **2004**, *126*, 10554–10555.
- (25) Mohadjer Beromi, M.; Banerjee, G.; Brudvig, G. W.; Hazari, N.; Mercado, B. Q. Nickel(I) Aryl Species: Synthesis, Properties, and Catalytic Activity. *ACS Catal.* **2018**, *8*, 2526–2533.
- (26) Dicciani, J. B.; Katigbak, J.; Hu, C.; Diao, T. Mechanistic Characterization of (Xantphos)Ni(I)-Mediated Alkyl Bromide Activation: Oxidative Addition, Electron Transfer, or Halogen-Atom Abstraction. *J. Am. Chem. Soc.* **2019**, *141*, 1788–1796.
- (27) Dicciani, J. B.; Hu, C. T.; Diao, T. Insertion of CO<sub>2</sub> Mediated by a (Xantphos)Ni(I)-Alkyl Species. *Angew. Chem., Int. Ed.* **2019**, *58*, 13865–13868.
- (28) Laskowski, C. A.; Bungum, D. J.; Baldwin, S. M.; Del Ciello, S. A.; Iluc, V. M.; Hillhouse, G. L. Synthesis and Reactivity of Two-Coordinate Ni(I) Alkyl and Aryl Complexes. *J. Am. Chem. Soc.* **2013**, *135*, 18272–18275.
- (29) Ciszewski, J. T.; Mikhaylov, D. Y.; Holin, K. V.; Kadirov, M. K.; Budnikova, Y. H.; Sinyashin, O.; Vivic, D. A. Redox Trends in Terpyridine Nickel Complexes. *Inorg. Chem.* **2011**, *50*, 8630–8635.
- (30) Schley, N. D.; Fu, G. C. Nickel-Catalyzed Negishi Arylations of Propargylic Bromides: A Mechanistic Investigation. *J. Am. Chem. Soc.* **2014**, *136*, 16588–16593.
- (31) Klein, A.; Kaiser, A.; Sarkar, B.; Wanner, M.; Fiedler, J. The Electrochemical Behaviour of Organonickel Complexes: Mono-, Di- and Trivalent Nickel. *Eur. J. Inorg. Chem.* **2007**, *2007*, 965–976.
- (32) Irwin, M.; Doyle, L. R.; Krämer, T.; Herchel, R.; McGrady, J. E.; Goicoechea, J. M. A Homologous Series of First-Row Transition-Metal Complexes of 2,2'-Bipyridine and their Ligand Radical Derivatives: Trends in Structure, Magnetism, and Bonding. *Inorg. Chem.* **2012**, *51*, 12301–12312.
- (33) Mohadjer Beromi, M.; Brudvig, G. W.; Hazari, N.; Lant, H. M. C.; Mercado, B. Q. Synthesis and Reactivity of Paramagnetic Nickel Polypyridyl Complexes Relevant to C(sp<sup>2</sup>)-C(sp<sup>3</sup>) Coupling Reactions. *Angew. Chem., Int. Ed.* **2019**, *58*, 6094–6098.
- (34) Somerville, R. J.; Odena, C.; Obst, M. F.; Hazari, N.; Hopmann, K. H.; Martin, R. Ni(I)-Alkyl Complexes Bearing Phenanthroline Ligands: Experimental Evidence for CO<sub>2</sub> Insertion at Ni(I) Centers. *J. Am. Chem. Soc.* **2020**, *142*, 10936–10941.
- (35) Yakhvarov, D. G.; Petr, A.; Kataev, V.; Büchner, B.; Gómez-Ruiz, S.; Hey-Hawkins, E.; Kvashennikova, S. V.; Ganushevich, Y. S.; Morozov, V. I.; Sinyashin, O. G. Synthesis, structure and electrochemical properties of the organonickel complex [NiBr(Mes)(phen)] (Mes = 2,4,6-trimethylphenyl, phen = 1,10-phenanthroline). *J. Organomet. Chem.* **2014**, *750*, 59–64.
- (36) Lin, Q.; Diao, T. Mechanism of Ni-Catalyzed Reductive 1,2-Dicarbofunctionalization of Alkenes. *J. Am. Chem. Soc.* **2019**, *141*, 17937–17948.
- (37) Dong, Q.; Zhao, Y.; Su, Y.; Su, J.-H.; Wu, B.; Yang, X.-J. Synthesis and Reactivity of Nickel Hydride Complexes of an  $\alpha$ -Diimine Ligand. *Inorg. Chem.* **2012**, *51*, 13162–13170.
- (38) Kuang, Y. L.; Anthony, D.; Katigbak, J.; Marrucci, F.; Humagain, S.; Diao, T. N. Ni(I)-Catalyzed Reductive Cyclization of 1,6-Dienes: Mechanism-Controlled trans Selectivity. *Chem.* **2017**, *3*, 268–280.
- (39) Zarate, C.; Yang, H.; Bezdek, M. J.; Hesk, D.; Chirik, P. J. Ni(I)-X Complexes Bearing a Bulky  $\alpha$ -Diimine Ligand: Synthesis, Structure, and Superior Catalytic Performance in the Hydrogen Isotope Exchange in Pharmaceuticals. *J. Am. Chem. Soc.* **2019**, *141*, 5034–5044.
- (40) Yin, H.; Fu, G. C. Mechanistic Investigation of Enantioconvergent Kumada Reactions of Racemic  $\alpha$ -Bromoketones Catalyzed by a Nickel/Bis(oxazoline) Complex. *J. Am. Chem. Soc.* **2019**, *141*, 15433–15440.
- (41) Yang, G.; Zhang, W. Renaissance of pyridine-oxazolines as chiral ligands for asymmetric catalysis. *Chem. Soc. Rev.* **2018**, *47*, 1783–1810.
- (42) Nganga, J. K.; Samanamu, C. R.; Tanski, J. M.; Pacheco, C.; Saucedo, C.; Batista, V. S.; Grice, K. A.; Ertem, M. Z.; Angeles-Boza, A. M. Electrochemical Reduction of CO<sub>2</sub> Catalyzed by Re(pyridine-oxazoline)(CO)<sub>3</sub>Cl Complexes. *Inorg. Chem.* **2017**, *56*, 3214–3226.
- (43) Lipschutz, M. I.; Yang, X.; Chatterjee, R.; Tilley, T. D. A Structurally Rigid Bis(amido) Ligand Framework in Low-Coordinate Ni(I), Ni(II), and Ni(III) Analogues Provides Access to a Ni(III) Methyl Complex via Oxidative Addition. *J. Am. Chem. Soc.* **2013**, *135*, 15298–15301.
- (44) Kundu, S.; Stieber, S. C. E.; Ferrier, M. G.; Kozimor, S. A.; Bertke, J. A.; Warren, T. H. Redox Non-Innocence of Nitrosobenzene at Nickel. *Angew. Chem., Int. Ed.* **2016**, *55*, 10321–10325.
- (45) Chirik, P. J.; Wieghardt, K. Radical Ligands Confer Nobility on Base-Metal Catalysts. *Science* **2010**, *327*, 794–795.
- (46) Neese, F. *Wiley Interdiscip. Rev.: Comput. Mol. Sci.* **2012**, *2*, 73.
- (47) Jana, R.; Pathak, T. P.; Sigman, M. S. Advances in Transition Metal (Pd,Ni,Fe)-Catalyzed Cross-Coupling Reactions Using Alkyl-organometallics as Reaction Partners. *Chem. Rev.* **2011**, *111*, 1417–1492.